ELSEVIER

Journal of Alloys and Compounds 281 (1998) 6–11

Journal of ALLOYS AND COMPOUNDS

Coercivity in lean rare earth NdFeB and PrFeB nanocomposite hard magnetic materials

S. David*, D. Givord

Laboratoire Louis Néel C.N.R.S., 25 avenue des Martyrs, BP 166, 38042 Grenoble Cedex, France

Abstract

NdFeB and PrFeB nanocomposite hard magnetic materials of the exchange-spring type were prepared by splat-cooling. Hysteresis cycles reveal that magnetisation processes may be analysed in terms of two contributions arising from the two different phases which exist in these systems. The soft phase magnetisation reverses first at a field of approximately 0.3 T which is found to be little temperature dependent. Reversal is determined by exchange coupling with the hard phase. A grain size of 20 nm is deduced. This value is in agreement with structural analysis. The hard-phase magnetisation reverses at a larger field value which is found to increase steadily with decreasing temperature (2.75 T in the PrFeB samples and 1.1 T in the NdFeB sample at 20 K). Reversal is found to be determined by processes which are reminiscent of those characterising reversal in usual sintered or melt-spun RFeB magnets. At room temperature, the activation volume deduced from magnetic after-effect measurements is 2200 nm^3. The contribution of inter-particle dipole interactions to magnetisation reversal is found to be small.

Keywords: Coercivity; Nanocomposite materials; RFeB magnets; Spring magnets

1. Introduction

Exchange-spring magnets constitute a new type of magnetic material in which a hard medium-magnetisation phase and a soft high-magnetisation phase are intimately intermixed [1]. Since the constituent crystallites are of nanometer size, exchange coupling between them allows combined high remanence and medium coercivity to be obtained. Ternary alloys with typical compositions $R_{4.5}Fe_{77.5}B_{18}$ (R=Nd, Pr,...) were the first category of exchange-spring magnets to be discovered [2]. Recently, several other systems were reported to exhibit the same type of properties [3–6].

Analysis of coercivity mechanisms in Nd–Fe–B hard magnets, sintered as well as prepared by melt-spinning, has recently been used in an attempt to try to find the subtle link which exists between coercivity and micro- or nano-structure. However, few such studies have been devoted to exchange-spring magnetic materials [7–9]. In the present paper, measurements of the temperature dependence of coercivity and magnetic viscosity in $Nd_4Fe_{78}B_{18}$ and $Pr_4Fe_{78}B_{18}$ nanocrystalline alloys (referred to as NdFeB and PrFeB in the rest of this article) are reported. The results are analysed within a model which has been previously applied to interpret coercivity in other hard magnetic materials [10].

2. Sample preparation and structural characterisation

The samples were prepared by splat-cooling. The experimental arrangement [11] used for this purpose includes a levitating high-frequency coil which is used to melt the desired alloy of typical weight 100 mg. When the alloy is liquid, the power is switched off, the liquid alloy drops and is intercepted by a rotating hammer and splat-cooled onto a facing anvil. The alloy cooling rate is approximately 10^7 $K\,s^{-1}$. In the present study, the alloy compositions were $Nd_4Fe_{78}B_{18}$ and $Pr_4Fe_{78}B_{18}$. X-ray analysis showed that the as-quenched alloys were amorphous. Two peaks were found to occur in DTA analysis at approximately 580 and 620°C with a 10 $K\,min^{-1}$ scanning rate. These could be associated with crystallisation of Fe on the one hand, and Fe_3B and $R_2Fe_{14}B$ on the other.

A small furnace in which two Kyocera resistors are closely assembled was used to flash-anneal the quenched samples. The temperature was raised to a maximum of typically 750°C, above the temperature of crystallisation of the different phases involved. The time required to reach the desired temperature was approximately 30 s. At that

*Corresponding author. E-mail: david@labs.polycnrs-gre.fr

0925-8388/98/$ – see front matter
PII: S0925-8388(98)00761-0

moment, the power was switched off. The sample temperature decreased very rapidly, in particular the decrease from 750 to 550°C, i.e. below the crystallisation temperature of the various phases mentioned above, was less than 15 s.

X-ray analysis of the annealed samples allowed the α-Fe and Fe_3B phases to be identified, however it was not possible to unambiguously detect the presence of the $R_2Fe_{14}B$ phase. Subsequent TEM analysis was performed at the TU Wien [12]. There, all the above three phases were identified. The mean crystallite size of the different phases was found to be extremely fine (typical dimensions 20 nm) and homogeneous.

3. Magnetic measurements

Magnetisation measurements were performed using a high-sensitivity VSM magnetometer equipped with a superconducting coil with maximum applied field 8 T and a range of accessible temperatures between 4.2 and 600 K.

3.1. Hysteresis cycles

Hysteresis cycles were measured at different temperatures from 300 down to 20 K (Fig. 1). At 300 K, the hysteresis cycles apparently indicate homogeneous reversal of the magnetisation. As the temperature is decreased a two-phase process becomes visible (in particular for PrFeB). The coercive field H_c^M may be defined as the field at which magnetisation vanishes. It should be noted that H_c^M exhibits a maximum around 150 K in NdFeB whereas, in PrFeB, a smooth increase is observed down to the lowest temperature (Fig. 2). The maximum in NdFeB may be related [7] to the spin-reorientation which takes place in $Nd_2Fe_{14}B$ at 135 K.

It must be stressed, however, that magnetisation reversal is characterised by irreversible phenomena and the above definition of the coercive field is not, in general, appropriate. A more physical definition of coercivity corresponds to the field at which irreversible processes are the largest [10]. The determination of this requires that reversible and irreversible processes be separated in the experimental hysteresis cycles. In order to extract the reversible susceptibility (χ_{rev}) contribution, measurements of recoil loops were performed at 20 mT field intervals. In general, significant time dependent magnetisation variations were found to occur at the field on the major cycle where the recoil loop was started. The measurements were taken after 100 s waiting time, when these effects had become negligible. χ_{rev} is found to peak at a field value which is approximately the same in both samples and varies from $\mu_0 H = 270$ mT at 300 K to 420 mT at 20 K (Figs. 3 and 4).

From χ_{rev} and the total susceptibility χ_{tot}, $\chi_{tot} - \chi_{rev}$ can be deduced. This term, although it is often identified as χ_{irr} is not strictly equal to it, and this is particularly the case

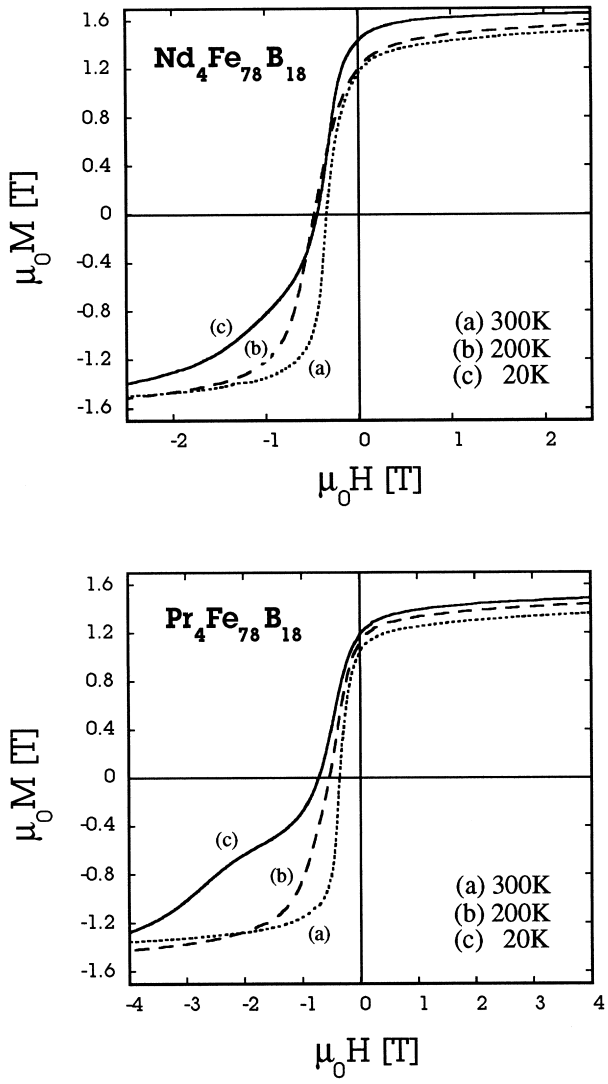

Fig. 1. $M(H)$ in $Nd_4Fe_{78}B_{18}$ and $Pr_4Fe_{78}B_{18}$ at (a) 300 K, (b) 200 K and (c) 20 K.

for exchange-spring systems where reversible and irreversible magnetisations are closely interrelated [13]. Nevertheless, the change in magnetisation represented by $\chi_{tot} - \chi_{rev}$ is predominantly associated with irreversible reversal phenomena. It is thus a meaningful quantity to characterise reversal. Its field variation in the studied samples is shown in Figs. 3 and 4. At a given temperature, a peak occurs in $(\chi_{tot} - \chi_{rev})(H)$. This peak may be defined as the coercive field, $H_c^{\chi_{tot}-\chi_{rev}}$, simply referred to as H_c [10]. In PrFeB, H_c increases by a factor of 6 as temperature decreases (from 380 mT at 300 K to 2.75 T at 20 K). In NdFeB, H_c increases in the same temperature range by only a factor of 3, from 360 mT at 300 K to 1.1 T at 20 K (Fig. 2). These variations resemble those observed in usual RFeB magnets, i.e. H_c monotonously increases as temperature is decreased, the low-temperature coercivity in the PrFeB sample, however, being significantly larger than in the NdFeB sample.

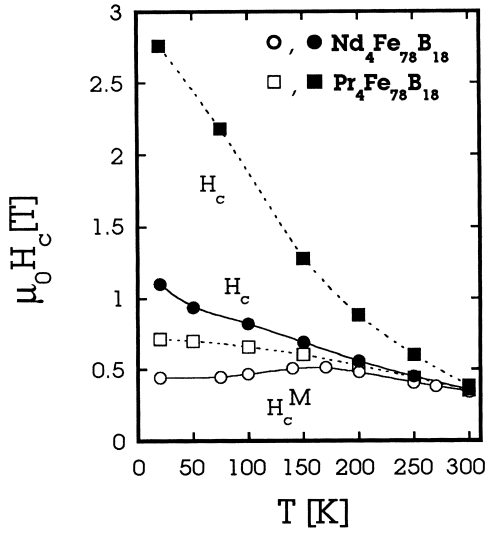

Fig. 2. $H_c^M(T)$ (empty symbols) and $H_c(T)$ (full symbols) in $Nd_4Fe_{78}B_{18}$ and $Pr_4Fe_{78}B_{18}$.

3.2. Reversal of the soft grain magnetisation: analysis of the temperature dependence of χ_{rev}

The above results indicate that reversal in the present systems may be separated into two distinct contributions, one representing soft phase reversal, which is essentially reversible and dominates at low field, and another representing hard phase reversal, which is essentially irreversible and dominates at high fields. Such a separation between the reversible and irreversible contributions is in agreement with previous analyses [8,14].

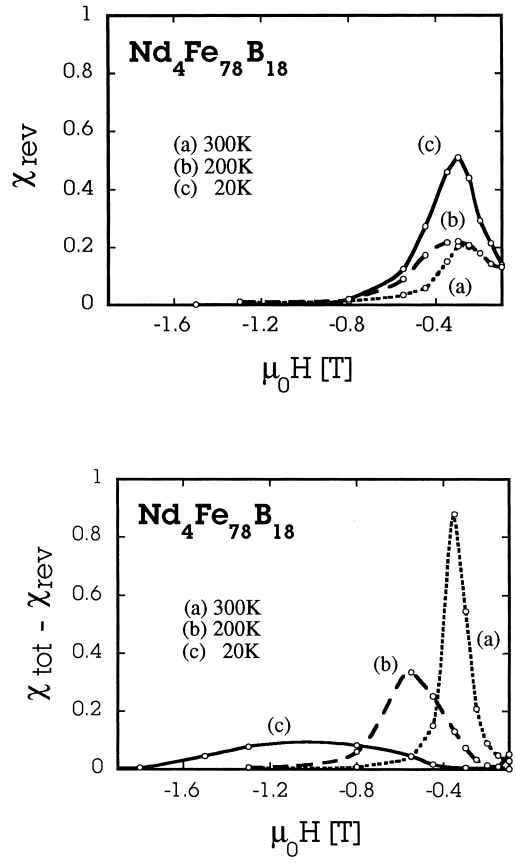

Fig. 3. χ_{rev} and $\chi_{tot} - \chi_{rev}$ in $Nd_4Fe_{78}B_{18}$ at (a) 300 K, (b) 200 K and (c) 20 K.

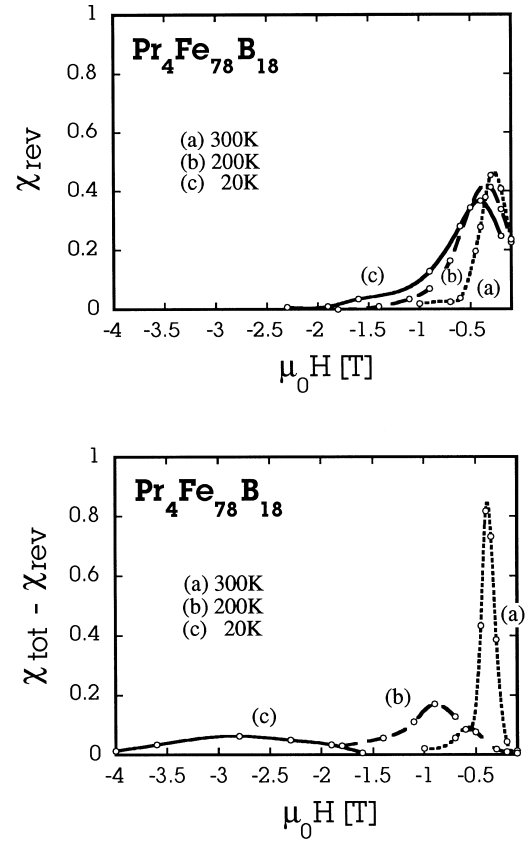

Fig. 4. χ_{rev} and $\chi_{tot} - \chi_{rev}$ in $Pr_4Fe_{78}B_{18}$ at (a) 300 K, (b) 200 K and (c) 20 K.

The maximum in χ_{rev} occurs at a field value which is much higher than the value expected for a soft magnetic phase. χ_{rev} is actually determined by interactions with the hard phase [1]. Reversal may be described in a semi-quantitative approach by assuming that the moment configuration in a soft grain is determined by the competition between Zeeman energy, which tends to align the moments along H, and exchange interactions, which favour their alignment along the moment direction in the adjacent hard grains. Assuming that the anisotropy in the hard grains is very large, the resulting moment configuration consists of a progressive rotation from an angle of maximum deviation, θ_{max}, in the centre of the soft grains, to alignment with the hard phase easy direction at the grain boundary with adjacent hard grains. To a first approximation, the stored exchange energy in a soft grain, exchange coupled with two hard grains with parallel magnetisation, may be expressed as

$$\gamma = (4A\theta_{max}^2)/d_{soft} \quad (1)$$

where A is the exchange constant and d_{soft} is the soft grain size. The Zeeman energy is

$$E_Z = \mu_0 M_s H(\sin\theta_{max}/\theta_{max}) d_{soft} \quad (2)$$

Minimisation yields for the field at which $\theta_{max} = \pi/2$ (corresponding approximately to reversal of half the soft phase, i.e. to the maximum of χ_{rev})

$$\mu_0 H = A\pi^3/2M_s d_{soft}^2 \quad (3)$$

The low temperature spontaneous magnetisation of the Fe_3B phase is $\mu_0 M_s = 1.65$ T and from $T_C = 785$ K, $A = 1.5\times10^{-11}$ J m^{-1} is deduced. At 20 K, the field at which χ_{rev} is maximum, $H_c^{\chi_{rev}}$, is 0.42 T in PrFeB (actually $H_c^{\chi_{rev}}$ is very close to H_c^M) which gives $d_{soft} = 20$ nm, in good agreement with TEM analysis.

The exchange constant A varies with temperature as M_s^2 and thus, from relation (3), $H_c^{\chi_{rev}}(T)$ should vary as M_s. In NdFeB, χ_{rev} is strongly influenced at low temperature by the magnetisation reorientation which takes place at 135 K and this makes difficult any quantitative comparison between experimental and calculated $H_c^{\chi_{rev}}(T)$. In PrFeB, however, the temperature dependence of $H_c^{\chi_{rev}}(T)$ also differs from the variation predicted by relation (3). It is actually much faster (see Fig. 5). For a soft grain surrounded by two hard grains with easy axes along the field and whose magnetisation is reversed, χ_{rev} should vanish. Thus a reduction in χ_{rev} is expected in the case where irreversible processes are superimposed on the reversible processes. At 300 K, the maximum in χ_{rev} is found at 0.28 T. At this field value, approximately 25% of the irreversible events have already occurred (see Fig. 4), and a reduction in χ_{rev} occurs which is of the same order of magnitude. It results that $H_c^{\chi_{rev}}$ is shifted to lower field where the influence of irreversible processes becomes negligible (Fig. 5).

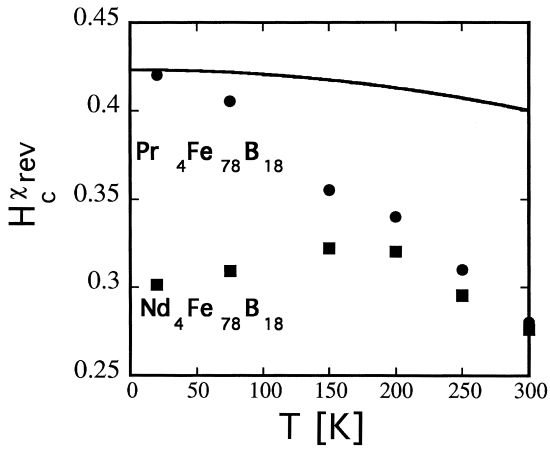

Fig. 5. $H_c^{\chi_{rev}}(T)$ in $Nd_4Fe_{78}B_{18}$ and $Pr_4Fe_{78}B_{18}$. The continuous line corresponds to $M_s(T)$ in Fe_3B calculated assuming that $M_s(T)/M_s(0)$ is the same as in Fe metal.

3.3. Reversal of the hard grain magnetisation: analysis of the temperature dependence of $\chi_{tot} - \chi_{rev}$

Magnetisation reversal in NdFeB sintered magnets as well as melt-spun materials was recently analysed within the so-called global model [10]. This model is based on the hypothesis that reversal is initiated in a small volume, the activation volume (v_a), under the influence of the external applied field, dipole interactions and thermal activation. The exact processes by which reversal takes place (nucleation, propagation or de-pinning) are not important in this discussion. It is actually thought that, in all cases, reversal is nucleated at some defect position through the initial formation of a local magnetisation heterogeneity. The basic simplifying assumptions are that the intrinsic physical properties at the defect position (anisotropy, exchange, magnetisation) are simply proportional to the same quantities in the bulk and that the corresponding proportionality coefficients are temperature independent. The coercive field is then derived as

$$\mu_0 H_c = \alpha\frac{\gamma}{M_s v_a^{1/3}} - N_{eff}\mu_0 M_s - \frac{25kT}{v_a M_s} \quad (4)$$

where γ is the domain wall energy. The activation volume, v_a, can be related to the experimental magnetic viscosity coefficient, S_v, through

$$v_a = \frac{kT}{\mu_0 S_v M_s} \quad (5)$$

with

$$S_v = \frac{S(1 - D\chi_{rev})}{\chi_{tot} - \chi_{rev}} \quad (6)$$

In relation (6), $S = dM/d\ln t$ is the time dependence of the magnetisation. S_v is usually derived from independent measurements of S and $\chi_{tot} - \chi_{rev}$. This procedure is very time consuming. In a simpler approach, S_v may be related to the shift in field, δH, between two magnetisation curves measured at respective waiting times, τ_1 and τ_2, after application of the field [15] (or to the shift in field between magnetisation curves measured at constant dM/dt [16]):

$$\delta H = S_v \ln(\tau_1/\tau_2) \quad (7)$$

$S_v(M)$ thus obtained at 300 and 100 K, for example, is shown in Fig. 6. It is found that S_v increases as magnetisation progressively reverses into the field direction. Such a field dependence of S_v is characteristic of heterogeneous systems.

The temperature dependence of S_v measured at the magnetisation value corresponding to H_c is shown in Fig. 7. The value of S_v obtained is approximately a factor of 5 smaller than in usual R–Fe–B magnets [10]. It is a well established experimental fact that S_v is approximately proportional to $H_c^{1.5}$ [17]. The present result is in qualitative agreement with this observation since the coercive

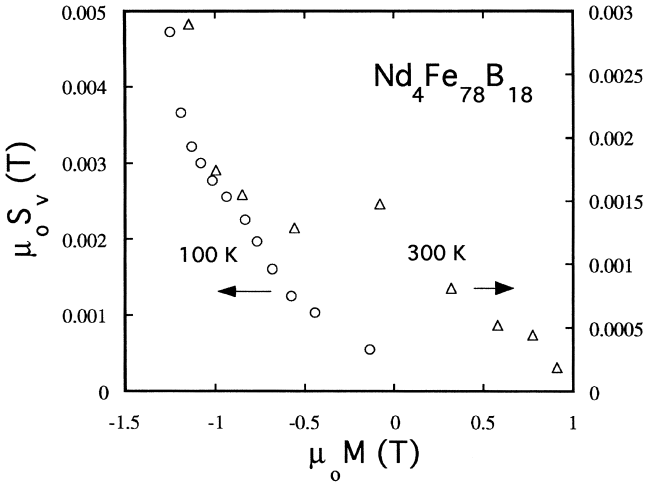

Fig. 6. $S_v(M)$ in $Nd_4Fe_{78}B_{18}$ at $T=100$ and 300 K.

field in usual R–Fe–B magnets is 3–5 times higher than in the spring-magnet materials. The temperature dependence of S_v as shown in Fig. 7 appears, in addition, to be strikingly similar to that observed in usual NdFeB magnets [10].

The activation volume, v_a, deduced from S_v is also shown in Fig. 7. v_a increases from approximately 100 nm^3 at 10 K to 2200 nm^3 at 300 K. At this latter temperature, v_a is comparable to the typical grain volume. Assuming a spherical activation volume, the corresponding diameter is about 16 nm; this is close to the average grain size (20 nm) found by TEM.

Once the activation volume is known, the coercive field, as expressed by relation (4), depends only on two parameters, α and N_{eff}. H_c/M_s as a function of $\gamma/M_s^2 v_a^{1/3}$ is shown in Fig. 8. A linear variation is observed for both the NdFeB and PrFeB systems, which indicates that the model applies. The parameter values deduced are $\alpha=0.28$ and $N_{eff}=0.05$ for $Nd_4Fe_{78}B_{18}$ and $\alpha=0.26$ and $N_{eff}=0.02$ for $Pr_4Fe_{78}B_{18}$. The value of the parameter α is smaller than in usual R–Fe–B magnets, which derives directly from the lower values of the coercive field in the spring magnets. The value of N_{eff} is close to 0. In sintered NdFeB magnets, $N_{eff}\approx 1$ is obtained, which indicates that large dipole interactions contribute to reversal. We suggest that the very small value of N_{eff} in the present system should be compared to the same result obtained in single phase melt-spun RFeB ribbons. On the one hand, it is expected that dipole interactions should decrease with the average grain size. On the other hand, it may be suggested that reversal mechanisms at the microscopic level show similarities in the different types of nanocrystallised NdFeB materials. In all cases, pinning may be favoured at the boundaries between hard grains (melt-spun NdFeB) or between a soft and a hard grain (spring magnets).

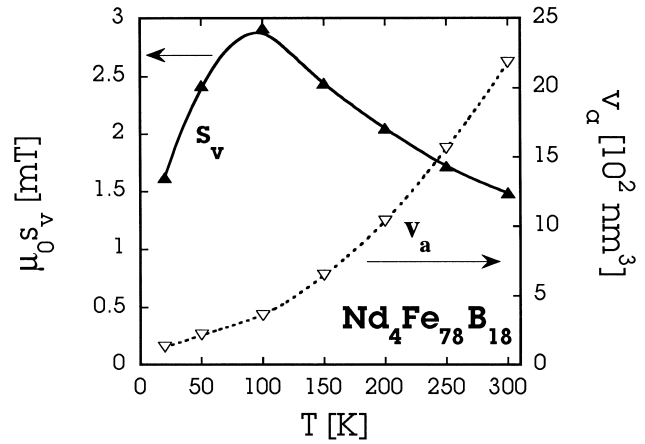

Fig. 7. $S_v(T)$ and $v_a(T)$ in $Nd_4Fe_{78}B_{18}$.

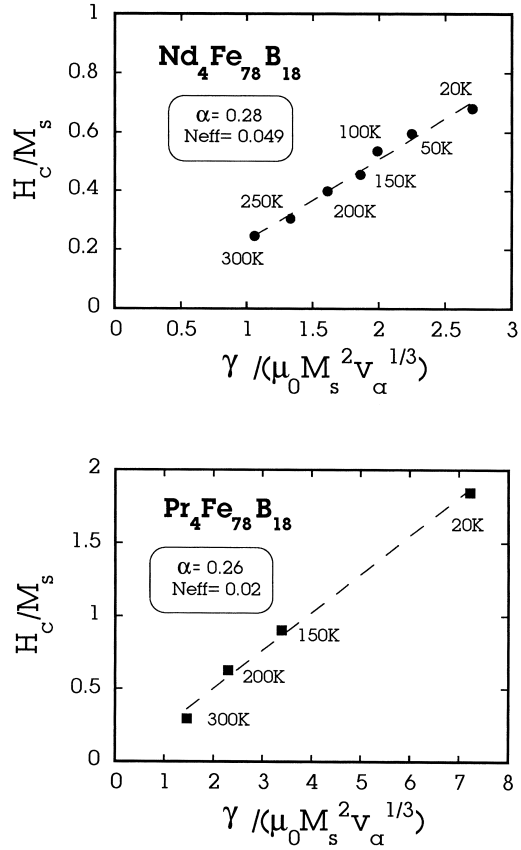

Fig. 8. H_c/M_s as a function of $\gamma/M_s^2 v_a^{1/3}$ in $Nd_4Fe_{78}B_{18}$ and $Pr_4Fe_{78}B_{18}$.

4. Conclusion

A semi-quantitative analysis of both reversible and irreversible processes in exchange-spring magnets has been presented in the present study. This allowed the essential physical parameters involved to be identified. Considering the complexity of these systems, a more quantitative approach requires numerical simulation to be performed. This has been developed, in particular, by Schrefl et al. [18]. In this case, however, the specific influence of each

parameter remains conjectural and needs to be compared carefully to experiment. This is why both approaches, phenomenological and numerical, have their own merit.

Acknowledgements

The support of the European Union within the Brite-Euram project EMERGE (No. BRPR-CT95-0097) is gratefully acknowledged.

References

[1] E.F. Kneller, R. Hawig, IEEE Trans. Magn. 27 (1991) 3588.
[2] R. Coehoorn, D.B. de Moij, J.P.W.B. Duchateau, K.H.J. Buschow, J. Phys. (Paris) C 8 (1988) 669; R. Coehoorn, C. de Waard, J. Magn. Magn. Mater. 83 (1990) 228.
[3] J. Ding, Y. Liu, P.G. McCormick, R. Street, J. Magn. Magn. Mater. 123 (1993) L239.
[4] V. Villas-Boas, S.A. Romero, F.P. Missel, in: Proceedings of the 9th International Symposium on Magnetic Anisotropy and Coercivity in RE–TM Alloys, São Paulo, 1996, Vol. 2, World Scientific, Singapore, 1996, p. 31.
[5] A. Manaf, R.A. Buckley, H.A. Davies, J. Magn. Magn. Mater. 128 (1993) 302.
[6] K. O'Donnell, C. Kuhrt, J.M.D. Coey, J. Appl. Phys. 76(10) (1994) 7068.
[7] D. Eckert, K.H. Müller, A. Handstein, J. Schneider, R. Grössinger, R. Krewenka, IEEE Trans. Magn. 26 (1990) 1834.
[8] E.H. Feutrill, P.G. McCormick, R. Street, J. Phys. D: Appl. Phys. 29 (1996) 2320.
[9] V. Patel, M. El-Hilo, K. O'Grady, R.W. Chantrell, J. Phys. D: Appl. Phys. 26 (1993) 1453.
[10] D. Givord, P. Tenaud, T. Viadieu, J. Appl. Phys. 60 (9) (1986) 3263; D. Givord, M.F. Rossignol, in: J.M.D. Coey (Ed.), Rare-earth Iron Permanent Magnets, Clarendon Press, Oxford, 1996, p. 218.
[11] S. David, W. Kiauka, D. Schmitt, R. Raphel (unpublished).
[12] The help of J. Bernardi and J. Fidler in TEM characterisation of the samples is gratefully acknowledged.
[13] R. Cammarano, P.G. McCormick, R. Street, J. Phys. D: Appl. Phys. 29 (1996) 2327.
[14] K.H. Müller, D. Eckert, A. Handstein, M. Wolf, L.L.M. Martinez, in: Proceedings of the 8th International Symposium on Magnetic Anisotropy and Coercivity in RE–TM Alloys, Birmingham, 1995, p. 179.
[15] D. Givord, M.F. Rossignol, V. Villas-Boas, F. Cebollada, J.M. Gonzalez, in: Proceedings of the 9th International Symposium on Magnetic Anisotropy and Coercivity in RE–TM Alloys, São Paulo, 1996, Vol. 2, World Scientific, Singapore, 1996, p. 21.
[16] R. Street, S.D. Brown, J. Appl. Phys. 76 (1994) 6386.
[17] J.C. Barbier, Ann. Phys. 9 (1954) 84.
[18] T. Schrefl, H. Roitner, J. Fidler, J. Appl. Phys. 81 (1997).